VIETNAM ACADEMY OF SCIENCE AND TECHNOLOGY

Vietnam Journal of MECHANICS

Volume 36 Number 1

ISSN 0866-7136

VN INDEX 12.666

1

2014

Vietnam Journal of Mechanics, VAST, Vol. 36, No. 1 (2014), pp. 61 – 75

DYNAMIC ANALYSIS OF MINDLIN PLATES ON VISCOELASTIC FOUNDATIONS UNDER A MOVING VEHICLE BY CS-MIN3 BASED ON C^0-TYPE HIGHER-ORDER SHEAR DEFORMATION THEORY

Nguyen Thoi Trung[1,2*], Phung Van Phuc[1], Tran Viet Anh[3], Nguyen Tran Chan[4]

[1] *Ton Duc Thang University, Ho Chi Minh City, Vietnam*

[2] *University of Science, VNU-HCMC, Vietnam*

[3] *SICOM Investment Construction JSC, Ho Chi Minh City, Vietnam*

[4] *Institute of Computational Engineering, Ho Chi Minh City, Vietnam*

[*] E-mail: nguyenthoitrung@tdt.edu.vn

Received May 06, 2013

Abstract. A cell-based smoothed three-node Mindlin plate element (CS-MIN3) based on the first-order shear deformation theory (FSDT) was recently proposed to improve the performance of the existing three-node Mindlin plate element (MIN3) for static and dynamics analyses of Mindlin plates. In this paper, the CS-MIN3 is extended to the C^0-type higher-order shear deformation plate theory (C^0-HSDT) and incorporated with damping-spring systems for dynamic analyses of Mindlin plates on the visco-elastic foundation subjected to a moving vehicle. The plate-foundation system is modeled as a discretization of triangular plate elements supported by discrete springs and dashpots at the nodal points representing the viscoelastic foundation. A two-step process for transforming the weight of a four-wheel vehicle into loads at nodes of elements is presented. The accuracy and reliability of the proposed method is verified by comparing its numerical solutions with those of others available numerical results. A parametric examination is also conducted to determine the effects of various parameters on the dynamic response of the plates on the viscoelastic foundation subjected to the moving vehicle.

Keywords: Smoothed finite element methods (S-FEM), Reissner-Mindlin plate, cell-based smoothed three-node Mindlin plate element (CS-MIN3), visco-elastic foundation, moving mass, moving vehicle.

1. INTRODUCTION

Dynamic response of Mindlin plates on visco-elastic foundations subjected to a moving vehicle can be found in several types of engineering structures and real life applications such as basement foundations of building, traffic highways, airport runways, etc. In general, loads on these type of structures are moving loads or moving masses such as the wheel loads from moving vehicles and planes.

Moving load problems were first studied to design the railroad bridges. Using experimental investigation and an analytical method, Ayre [1] first analyzed the moving load problems for the design of one and two-span beams. Using the finite element method (FEM), Yoshida and Weaver [2] investigated the dynamic response of simply supported beams and plates to moving force and moving mass loads. In this work, the moving mass problem was approximated by a simplified pavement model that accounts for the dynamic interaction between the vehicle and the pavement. Extending the moving load problems to the dynamic analysis of the beams on elastic or viscoelatic foundations, Kenney [3] first analyzed the dynamic response of an infinitely long Bernoulli-Euler beam on a Winkler foundation subjected to a moving force, including the effects of linear damping. In this study, the subgrade was idealized as a Winkler medium which does not account for the continuous nature of the actual subgrade. Further extending the moving load problems to the dynamic analysis of the plates on elastic foundations, Thompson [4] carried out a dynamic analysis of roads subjected to longitudinally moving loads by assuming the pavement as an infinitely long thin plate. Related to the dynamic analysis of the plates on viscoelastic foundations, Zaman [5] used the four-node elements in the FEM to analyze dynamic response of a thick plate on viscoelastic foundation to moving loads by taking into account the transverse shear deformation as well as bending of the slab. Sun [6] established a closed form solution by using the Fourier transformation to derive the analytical dynamic solution of a Kirchhoff plate on a viscoelastic foundation to harmonic circular loads.

In comparison, it is seen that many studies in the literature have concerned with the dynamic analysis of plates on elastic foundations subjected to moving loads, while the literature related to those of plates on viscoelastic foundations is somewhat still limited. This paper hence aims to further contribute a dynamic analysis of Mindlin plates on viscoelastic foundations subjected to a moving vehicle. The method used here is still the FEM, however the elements used are triangular elements which are different from the four-node quadrilateral elements used in Ref [5].

In the other frontier of developing advanced finite element technologies, Liu and Nguyen-Thoi [7] have applied a strain smoothing technique of meshfree methods by Chen [8] into the conventional FEM using linear interpolations to formulate a series of smoothed finite element methods (S-FEM) including the cell-based smoothed FEM (CS-FEM) [9] which shows some interesting properties in the solid mechanics problems. The S-FEM models have also been further investigated and applied to various problems such as plates and shells [10–15], piezoelectricity [16] and some other applications [17, 18], etc. Extending the idea of the CS-FEM to plate structures, Nguyen-Thoi et al. [19] have recently formulated a cell-based smoothed three-node Mindlin plate element (CS-MIN3) for static, and free vibration analyses of isotropic Mindlin plates by incorporating the CS-FEM with the original MIN3 element [20]. In the CS-MIN3, each triangular element will be divided into three sub-triangles, and in each sub-triangle, the stabilized MIN3 is used to compute the strains. Then the strain smoothing technique on whole the triangular element is used to smooth the strains on these three sub-triangles. The numerical results showed that the CS-MIN3 is free of shear locking and achieves the high accuracy.

This paper hence extends the triangular plate element CS-MIN3 based on C^0-type higher-order shear deformation theory (C^0-HSDT) for dynamic analyses of Mindlin plates on visco-elastic foundation subjected to a moving vehicle. The plate-foundation system is modeled as a discretization of triangular plate elements supported by discrete springs and dashpots at the nodal points representing the viscoelastic foundation. A two-step process for transforming the weight of a four-wheel vehicle into loads at nodes of elements will be presented. The accuracy and reliability of the proposed method will be verified by comparing its numerical solutions with those of others available numerical results. A parametric examination will be conducted to determine the effects of various parameters on the dynamic response of the plates on the viscoelastic foundation subjected to the moving vehicle.

2. A C^0-TYPE HIGHER-ORDER SHEAR DEFORMATION THEORY AND WEAKFORM FOR MINDLIN PLATES ON VISCOELASTIC FOUNDATION

2.1. C^0-type higher-order shear deformation theory (C^0-HSDT)

According to C^0-HSDT model [21], the displacements of an arbitrary point in the plate are expressed by

$$\begin{aligned} u(x,y,z) &= u_0 + \left(z - \frac{4z^3}{3t^2}\right)\beta_x - \frac{4z^3}{3t^2}\varphi_x, \\ v(x,y,z) &= v_0 + \left(z - \frac{4z^3}{3t^2}\right)\beta_y - \frac{4z^3}{3t^2}\varphi_y \quad (-t/2 \le z \le t/2), \\ w(x,y) &= w, \end{aligned} \tag{1}$$

where t is thickness of plate; $\mathbf{u}_0 = \{u_0\ v_0\}^T$, w and $\boldsymbol{\beta} = \{\beta_x\ \beta_y\}^T$ are the membrane displacements, the transverse displacement of the mid-plane and the rotations in the $y-z, x-z$ planes respectively.

Eq. (1) is developed from Reddy's higher-order theory [22], in which, the derivative of deflection is replaced by warping function $\boldsymbol{\phi} = \{\phi_x\ \phi_y\}^T$. Thus, the generalized displacement vector with 5 degrees of freedom (DOFs) for C^1 continuity element is transformed into the vector with 7 DOFs for C^0 continuity element as $\mathbf{u} = \left[\begin{array}{ccccccc} u_0 & v_0 & w & \beta_x & \beta_y & \phi_x & \phi_y \end{array}\right]^T$

$$\left[\begin{array}{ccc} \varepsilon_{xx} & \varepsilon_{yy} & \gamma_{xy} \end{array}\right]^T = \boldsymbol{\varepsilon}_0 + z\boldsymbol{\kappa}_1 + z^3\boldsymbol{\kappa}_2 \tag{2}$$

and the bending strains are given by

$$\begin{aligned} \boldsymbol{\kappa}_1 &= \frac{1}{2}\left\{\nabla\boldsymbol{\beta} + (\nabla\boldsymbol{\beta})^T\right\} \\ \boldsymbol{\kappa}_2 &= \frac{\mathrm{c}}{6}\left\{\left(\nabla\boldsymbol{\phi} + (\nabla\boldsymbol{\phi})^T\right) + \left(\nabla\boldsymbol{\beta} + (\nabla\boldsymbol{\beta})^T\right)\right\} \end{aligned} \quad \text{with} \quad c = -\frac{4}{t^2} \tag{3}$$

and transverse shear strains are basically defined as

$$[\gamma_{xz}\ \gamma_{yz}]^T = \boldsymbol{\varepsilon}_s + z^2\boldsymbol{\kappa}_s \text{ with } \boldsymbol{\varepsilon}_s = \nabla w + \boldsymbol{\beta}\ ; \quad \boldsymbol{\kappa}_s = c\,(\boldsymbol{\beta} + \boldsymbol{\phi}) \tag{4}$$

where $\nabla = [\partial/\partial x\ \partial/\partial y]^T$ is the gradient operator.

The transverse shear strains in Eq. (4) is represented parabolically. It is clear that the shear correction factors can be removed in the C^0-HSDT formulation [21].

2.2. Weak form for Mindlin plates on viscoelastic foundation

Consider a Mindlin plate on viscoelastic foundation as shown in Fig. 1a. The viscoelastic foundation is modeled by discrete springs with foundation stiffness coefficient k_f and dampings with damping coefficients c_f.

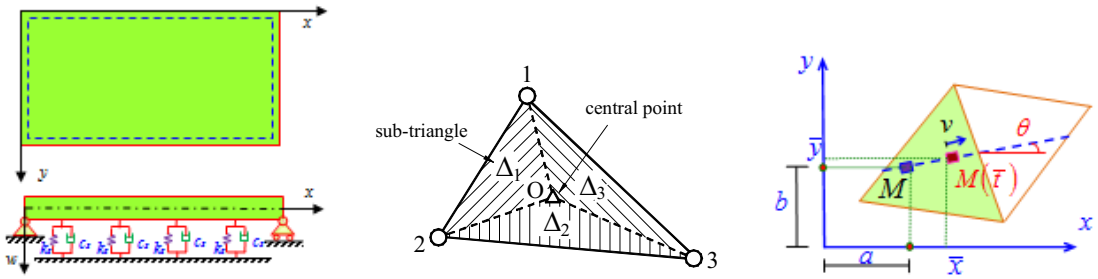

(a) (b) (c)

Fig. 1. (a) Model of a Mindlin thick plate on viscoelastic foundation; (b) Three sub-triangles (Δ_1, Δ_2 and Δ_3) created from the triangle 1-2-3 in the CS-MIN3 by connecting the central point O with three field nodes 1, 2 and 3; (c) Position of a moving mass crossing triangular elements

The standard Galerkin weak form of the transient analysis of Mindlin plates on viscoelastic foundation can be written as [5]

$$\int_\Omega \delta\boldsymbol{\varepsilon}_p^T \mathbf{D}^* \boldsymbol{\varepsilon}_p \mathrm{d}\Omega + \int_\Omega \delta\boldsymbol{\gamma}^T \mathbf{D}_S^* \boldsymbol{\gamma} \mathrm{d}\Omega + \int_\Omega \delta\mathbf{u}^T \mathbf{m}\, \ddot{\mathbf{u}} \mathrm{d}\Omega + \int_\Omega \delta w^T k_f w \,\mathrm{d}\Omega + \int_\Omega \delta w^T c_f \dot{w} \,\mathrm{d}\Omega = \int_\Omega \delta\mathbf{u}^T \mathbf{b} \,\mathrm{d}\Omega \tag{5}$$

where $\mathbf{b}$ is the distributed load applied on the plate, and strain components $\boldsymbol{\varepsilon}_p$ and $\boldsymbol{\gamma}$ are expressed by

$$\boldsymbol{\varepsilon}_p = \left\{ \begin{array}{ccc} \boldsymbol{\varepsilon}_0 & \boldsymbol{\kappa}_1 & \boldsymbol{\kappa}_2 \end{array} \right\}^T, \quad \boldsymbol{\gamma} = \left\{ \begin{array}{cc} \boldsymbol{\varepsilon}_s & \boldsymbol{\kappa}_s \end{array} \right\}^T \tag{6}$$

and material constant matrices $\mathbf{D}^*$ and $\mathbf{D}_S^*$ have the forms of

$$\mathbf{D}^* = \begin{bmatrix} \mathbf{A} & \mathbf{B} & \mathbf{E} \\ \mathbf{B} & \mathbf{D} & \mathbf{F} \\ \mathbf{E} & \mathbf{F} & \mathbf{H} \end{bmatrix}, \quad \mathbf{D}_S^* = \begin{bmatrix} \mathbf{A}^S & \mathbf{B}^S \\ \mathbf{B}^S & \mathbf{D}^S \end{bmatrix}, \tag{7}$$

where

$$\begin{aligned} (\mathbf{A}_{ij}, \mathbf{B}_{ij}, \mathbf{D}_{ij}, \mathbf{E}_{ij}, \mathbf{F}_{ij}, \mathbf{H}_{ij}) &= \int_{-h/2}^{h/2} \left(1, z, z^2, z^3, z^4, z^6\right) \bar{Q}_{ij} \mathrm{d}z \quad i,j = 1,2,6 \\ \left(\mathbf{A}_{ij}^s, \mathbf{B}_{ij}^s, \mathbf{D}_{ij}^s\right) &= \int_{-h/2}^{h/2} \left(1, z^2, z^4\right) \bar{Q}_{ij} \mathrm{d}z \quad i,j = 4,5 \end{aligned} \tag{8}$$

and $\mathbf{m}$ is the matrix containing the mass density of the material ρ and thickness t as

$$\mathbf{m} = \begin{bmatrix} I_1 & 0 & 0 & I_2 & 0 & c/3I_4 & 0 \\ & I_1 & 0 & 0 & I_2 & 0 & c/3I_4 \\ & & I_1 & 0 & 0 & 0 & 0 \\ & & & I_3 & 0 & c/3I_5 & 0 \\ & & & & I_3 & 0 & c/3I_5 \\ & & & & & c^2/9I_7 & 0 \\ sym & & & & & & c^2/9I_7 \end{bmatrix} \tag{9}$$

with $(I_1, I_2, I_3, I_4, I_5, I_7) = \int_{-t/2}^{t/2} \rho \left(1, z, z^2, z^3, z^4, z^6\right) \mathrm{d}z$.

3. FORMULATION OF THE CS-MIN3 FOR MINDLIN PLATES ON VISCOELASTIC FOUNDATION

3.1. FEM formulation for Mindlind plates on viscoelastic foundation [5]

Now, discretize the bounded domain Ω into N_e finite elements such that $\Omega = \bigcup_{e=1}^{N_e} \Omega_e$ and $\Omega_i \cap \Omega_j = \emptyset$, $i \neq j$, then the finite element solution $\mathbf{u}^h = [\ u_0 \quad v_0 \quad w \quad \beta_x \quad \beta_y \quad \phi_x \quad \phi_y]^T$ of a displacement model for the Mindlin plates is expressed as

$$\mathbf{u}^h = \sum_{I=1}^{N_n} diag\left[N_I(\mathbf{x}),\ N_I(\mathbf{x}),\ N_I(\mathbf{x}),\ N_I(\mathbf{x}),\ N_I(\mathbf{x}),\ N_I(\mathbf{x}),\ N_I(\mathbf{x})\right]\mathbf{d}_I = \mathbf{N}\mathbf{d} \tag{10}$$

where N_n is the total number of nodes of problem domain discretized; $N_I(\mathbf{x})$ is shape function at node I; $\mathbf{d}_I = [\ u_I \quad v_I \quad w_I \quad \beta_{xI} \quad \beta_{yI} \quad \phi_{xI} \quad \phi_{yI}]^T$ is the displacement vector of the nodal degrees of freedom of $\mathbf{u}^h$ associated to node I, respectively.

Substituting Eq. (10) into Eq. (6), then the strains in Eq. (6) can be expressed as

$$\boldsymbol{\varepsilon}^h = [\boldsymbol{\varepsilon}_p \quad \boldsymbol{\gamma}]^T = \sum_{I=1}^{N_n} \mathbf{B}_I^* \mathbf{d}_I \tag{11}$$

where $\boldsymbol{\varepsilon}^h$ is the compatible strain and $\mathbf{B}_I^*$ is the generalized strain-displacement matrix expressed by

$$\mathbf{B}_I^* = \left[(\mathbf{B}_I^m)^T \quad \left(\mathbf{B}_I^{b_1}\right)^T \quad \left(\mathbf{B}_I^{b_2}\right)^T \quad \left(\mathbf{B}_I^{s_0}\right)^T \quad \left(\mathbf{B}_I^{s_1}\right)^T\right] \tag{12}$$

in which

$$\mathbf{B}_I^m = \begin{bmatrix} N_{I,x} & 0 & 0 & 0 & 0 & 0 & 0 \\ 0 & N_{I,y} & 0 & 0 & 0 & 0 & 0 \\ N_{I,y} & N_{I,x} & 0 & 0 & 0 & 0 & 0 \end{bmatrix}, \quad \mathbf{B}_I^{b_1} = \begin{bmatrix} 0 & 0 & 0 & N_{I,x} & 0 & 0 & 0 \\ 0 & 0 & 0 & 0 & N_{I,y} & 0 & 0 \\ 0 & 0 & 0 & N_{I,y} & N_{I,x} & 0 & 0 \end{bmatrix}$$

$$\mathbf{B}_I^{b_2} = \frac{c}{3}\begin{bmatrix} 0 & 0 & 0 & N_{I,x} & 0 & N_{I,x} & 0 \\ 0 & 0 & 0 & 0 & N_{I,y} & 0 & N_{I,y} \\ 0 & 0 & 0 & N_{I,y} & N_{I,x} & N_{I,y} & N_{I,x} \end{bmatrix} \tag{13}$$

$$\mathbf{B}_I^{s_0} = \begin{bmatrix} 0 & 0 & N_{I,x} & N_I & 0 & 0 & 0 \\ 0 & 0 & N_{I,y} & 0 & N_I & 0 & 0 \end{bmatrix}, \quad \mathbf{B}_I^{s_1} = c\begin{bmatrix} 0 & 0 & 0 & N_I & 0 & N_I & 0 \\ 0 & 0 & 0 & 0 & N_I & 0 & N_I \end{bmatrix}$$

in which $N_{I,x}$ and $N_{I,y}$ are the derivatives of the shape functions in x-direction and y-direction, respectively. The discretized system of equations of Mindlin plates on viscoelastic foundation using the FEM for transient analysis then can be expressed as

$$\mathbf{M}\ddot{\mathbf{d}} + \mathbf{C}\dot{\mathbf{d}} + \mathbf{K}\mathbf{d} = \mathbf{F} \tag{14}$$

where $\mathbf{K}$ is the global stiffness matrix given by

$$\mathbf{K} = \int_{\Omega} \mathbf{B}^T \mathbf{D}^* \mathbf{B} \mathrm{d}\Omega + \int_{\Omega} \mathbf{S}^T \mathbf{D}_s^* \mathbf{S} \mathrm{d}\Omega + \int_{\Omega} {\mathbf{N}_w}^T k_f \mathbf{N}_w \, \mathrm{d}\Omega \tag{15}$$

in which $\mathbf{N}_w = [0\ 0\ N_1\ 0\ 0\ 0\ 0\ 0\ 0\ N_2\ 0\ 0\ 0\ 0\ 0\ 0\ N_3\ 0\ 0\ 0\ 0]$; $\mathbf{F}$ is the load vector defined by

$$\mathbf{F} = \int_{\Omega} p\mathbf{N} \, d\Omega + \mathbf{f}^b \tag{16}$$

in which $\mathbf{f}^b$ is the remaining part of $\mathbf{F}$ subjected to prescribed boundary loads; $\mathbf{M}$ and $\mathbf{C}$ are the global mass and global damping matrices defined by

$$\mathbf{M} = \int_{\Omega} \mathbf{N}^T \mathbf{m} \mathbf{N} \mathrm{d}\Omega \ \text{ and } \ \mathbf{C} = \int_{\Omega} \mathbf{N}_w^T c_f \mathbf{N}_w \mathrm{d}\Omega \tag{17}$$

3.2. Formulation of CS-MIN3 for Mindlin plates on viscoelastic foundation

In the CS-MIN3 [10], the domain discretization is the same as that of the MIN3 using N_n nodes and N_e triangular elements. However in the formulation of the CS-MIN3, each triangular element Ω_e is further divided into three sub-triangles Δ_1, Δ_2 and Δ_3 by connecting the central point 0 of the element to three field nodes as shown in Fig. 1b.

In the CS-MIN3, we assume that the displacement vector $\mathbf{d}_{e0}$ at the central point 0 is the simple average of three displacement vectors $\mathbf{d}_{e1}$, $\mathbf{d}_{e2}$ and $\mathbf{d}_{e3}$ of three field nodes

$$\mathbf{d}_{e0} = \frac{1}{3}\left(\mathbf{d}_{e1} + \mathbf{d}_{e2} + \mathbf{d}_{e3}\right) \tag{18}$$

Using the MIN3 formulation [20] for the sub-triangle Δ_1, the bending and shear strains $\boldsymbol{\kappa}^{\Delta_1}$ and $\boldsymbol{\gamma}^{\Delta_1}$ can be approximated by

$$\boldsymbol{\varepsilon}_0^{\Delta_1} = \underbrace{\left[\begin{array}{ccc} \mathbf{b}_1^{m\Delta_1} & \mathbf{b}_2^{m\Delta_1} & \mathbf{b}_3^{m\Delta_1} \end{array}\right]}_{\mathbf{b}^{m\Delta_1}} \left[\begin{array}{c} \mathbf{d}_{e0} \\ \mathbf{d}_{e1} \\ \mathbf{d}_{e2} \end{array}\right] = \mathbf{b}^{m\Delta_1}\mathbf{d}^{\Delta_1} \tag{19}$$

$$\begin{aligned} \boldsymbol{\kappa}_1^{\Delta_1} &= \underbrace{\left[\begin{array}{ccc} \mathbf{b}_1^{b_1\Delta_1} & \mathbf{b}_2^{b_1\Delta_1} & \mathbf{b}_3^{b_1\Delta_1} \end{array}\right]}_{\mathbf{b}^{b_1\Delta_1}} \left[\begin{array}{c} \mathbf{d}_{e0} \\ \mathbf{d}_{e1} \\ \mathbf{d}_{e2} \end{array}\right] = \mathbf{b}^{b_1\Delta_1}\mathbf{d}^{\Delta_1}; \\ \boldsymbol{\kappa}_2^{\Delta_1} &= \underbrace{\left[\begin{array}{ccc} \mathbf{b}_1^{b_2\Delta_1} & \mathbf{b}_2^{b_2\Delta_1} & \mathbf{b}_3^{b_2\Delta_1} \end{array}\right]}_{\mathbf{b}^{b_2\Delta_1}} \left[\begin{array}{c} \mathbf{d}_{e0} \\ \mathbf{d}_{e1} \\ \mathbf{d}_{e2} \end{array}\right] = \mathbf{b}^{b_2\Delta_1}\mathbf{d}^{\Delta_1} \end{aligned} \tag{20}$$

$$\begin{aligned}
\boldsymbol{\varepsilon}_s^{\Delta_1} &= \underbrace{\left[\begin{array}{ccc} \mathbf{b}_1^{s_0\Delta_1} & \mathbf{b}_2^{s_0\Delta_1} & \mathbf{b}_3^{s_0\Delta_1} \end{array}\right]}_{\mathbf{b}^{s_0\Delta_1}} \left[\begin{array}{c} \mathbf{d}_{e0} \\ \mathbf{d}_{e1} \\ \mathbf{d}_{e2} \end{array}\right] = \mathbf{b}^{s_0\Delta_1}\mathbf{d}^{\Delta_1}; \\
\boldsymbol{\kappa}_s^{\Delta_1} &= \underbrace{\left[\begin{array}{ccc} \mathbf{b}_1^{s_1\Delta_1} & \mathbf{b}_2^{s_1\Delta_1} & \mathbf{b}_3^{s_1\Delta_1} \end{array}\right]}_{\mathbf{b}^{s_1\Delta_1}} \left[\begin{array}{c} \mathbf{d}_{e0} \\ \mathbf{d}_{e1} \\ \mathbf{d}_{e2} \end{array}\right] = \mathbf{b}^{s_1\Delta_1}\mathbf{d}^{\Delta_1}
\end{aligned} \tag{21}$$

where $\mathbf{b}^{m\Delta_1}$, $\mathbf{b}^{b_1\Delta_1}$, $\mathbf{b}^{b_2\Delta_1}$, $\mathbf{b}^{s_0\Delta_1}$ and $\mathbf{b}^{s_1\Delta_1}$ are, respectively, computed similarly as the matrices $\mathbf{B}^m$, $\mathbf{B}^{b_1}$, $\mathbf{B}^{b_2}$, $\mathbf{B}^{s_0}$ and $\mathbf{B}^{s_1}$ of the MIN3 [20]. Substituting $\mathbf{d}_0^e$ in Eq. (18) into Eqs. (19), (20) and (21), and then rearranging we obtain

$$\boldsymbol{\varepsilon}_0^{\Delta_1} = \underbrace{\left[\begin{array}{ccc} \frac{1}{3}\mathbf{b}_1^{m\Delta_1} + \mathbf{b}_2^{m\Delta_1} & \frac{1}{3}\mathbf{b}_1^{m\Delta_1} + \mathbf{b}_3^{m\Delta_1} & \frac{1}{3}\mathbf{b}_1^{m\Delta_1} \end{array}\right]}_{\mathbf{B}^{m\Delta_1}} [\mathbf{d}_{e0}\ \mathbf{d}_{e1}\ \mathbf{d}_{e2}]^T = \mathbf{B}^{m\Delta_1}\mathbf{d}^{\Delta_1} \tag{22}$$

$$\begin{aligned}
\boldsymbol{\kappa}_1^{\Delta_1} &= \underbrace{\left[\begin{array}{ccc} \frac{1}{3}\mathbf{b}_1^{b_1\Delta_1} + \mathbf{b}_2^{b_1\Delta_1} & \frac{1}{3}\mathbf{b}_1^{b_1\Delta_1} + \mathbf{b}_3^{b_1\Delta_1} & \frac{1}{3}\mathbf{b}_1^{b_1\Delta_1} \end{array}\right]}_{\mathbf{B}^{b_1\Delta_1}} [\mathbf{d}_{e0}\ \mathbf{d}_{e1}\ \mathbf{d}_{e2}]^T = \mathbf{B}^{b_1\Delta_1}\mathbf{d}^{\Delta_1} \\
\boldsymbol{\kappa}_2^{\Delta_1} &= \underbrace{\left[\begin{array}{ccc} \frac{1}{3}\mathbf{b}_1^{b_2\Delta_1} + \mathbf{b}_2^{b_2\Delta_1} & \frac{1}{3}\mathbf{b}_1^{b_2\Delta_1} + \mathbf{b}_3^{b_2\Delta_1} & \frac{1}{3}\mathbf{b}_1^{b_2\Delta_1} \end{array}\right]}_{\mathbf{B}^{b_2\Delta_1}} [\mathbf{d}_{e0}\ \mathbf{d}_{e1}\ \mathbf{d}_{e2}]^T = \mathbf{B}^{b_2\Delta_1}\mathbf{d}^{\Delta_1}
\end{aligned} \tag{23}$$

$$\begin{aligned}
\boldsymbol{\varepsilon}_s^{\Delta_1} &= \underbrace{\left[\begin{array}{ccc} \frac{1}{3}\mathbf{b}_1^{s_0\Delta_1} + \mathbf{b}_2^{s_0\Delta_1} & \frac{1}{3}\mathbf{b}_1^{s_0\Delta_1} + \mathbf{b}_4^{s_0\Delta_1} & \frac{1}{3}\mathbf{b}_1^{s_0\Delta_1} \end{array}\right]}_{\mathbf{B}^{s_0\Delta_1}} [\mathbf{d}_{e0}\ \mathbf{d}_{e1}\ \mathbf{d}_{e2}]^T = \mathbf{B}^{s_0\Delta_1}\mathbf{d}^{\Delta_1} \\
\boldsymbol{\kappa}_s^{\Delta_1} &= \underbrace{\left[\begin{array}{ccc} \frac{1}{3}\mathbf{b}_1^{s_1\Delta_1} + \mathbf{b}_2^{s_1\Delta_1} & \frac{1}{3}\mathbf{b}_1^{s_1\Delta_1} + \mathbf{b}_3^{s_1\Delta_1} & \frac{1}{3}\mathbf{b}_1^{s_1\Delta_1} \end{array}\right]}_{\mathbf{B}^{s_1\Delta_1}} [\mathbf{d}_{e0}\ \mathbf{d}_{e1}\ \mathbf{d}_{e2}]^T = \mathbf{B}^{s_1\Delta_1}\mathbf{d}^{\Delta_1}
\end{aligned} \tag{24}$$

Similarly, by using cyclic permutation, we easily obtain the bending and shear strains $\boldsymbol{\varepsilon}_0^{\Delta_j}$, $\boldsymbol{\kappa}_1^{\Delta_j}$, $\boldsymbol{\kappa}_2^{\Delta_j}, \boldsymbol{\varepsilon}_s^{\Delta_j}$, $\boldsymbol{\kappa}_s^{\Delta_j}$ and matrices $\mathbf{B}^{m\Delta_j}$, $\mathbf{B}^{b_1\Delta_j}$, $\mathbf{B}^{b_2\Delta_j}$, $\mathbf{B}^{s_0\Delta_j}$, $\mathbf{B}^{s_1\Delta_j}$, $j = 2, 3$, for the second sub-triangle Δ_2 (triangle 0-2-3) and third sub-triangle Δ_3 (triangle 0-3-1), respectively.

Now, applying the cell-based strain smoothing operation in the CS-FEM [7], the constant bending and shear strains $\boldsymbol{\kappa}^{\Delta_j}$ and $\boldsymbol{\gamma}^{\Delta_j}$, $j = 1, 2, 3$ are, respectively, used to create a *smoothed* bending and shear strains $\tilde{\boldsymbol{\kappa}}_e$ and $\tilde{\boldsymbol{\gamma}}_e$ on the element Ω_e such as

$$\begin{aligned}
\tilde{\boldsymbol{\varepsilon}}_{e0} = \frac{1}{A_e}\sum_{j=1}^{3} A_{\Delta_j}\boldsymbol{\varepsilon}_0^{\Delta_j};\ \tilde{\boldsymbol{\kappa}}_{e1} = \frac{1}{A_e}\sum_{j=1}^{3} A_{\Delta_j}\boldsymbol{\kappa}_1^{\Delta_j};\ \tilde{\boldsymbol{\kappa}}_{e2} = \frac{1}{A_e}\sum_{j=1}^{3} A_{\Delta_j}\boldsymbol{\kappa}_2^{\Delta_j}; \\
\tilde{\boldsymbol{\varepsilon}}_{es} = \frac{1}{A_e}\sum_{j=1}^{3} A_{\Delta_j}\boldsymbol{\varepsilon}_s^{\Delta_j};\ \tilde{\boldsymbol{\kappa}}_{es} = \frac{1}{A_e}\sum_{j=1}^{3} A_{\Delta_j}\boldsymbol{\kappa}_s^{\Delta_j}
\end{aligned} \tag{25}$$

where $\tilde{\mathbf{B}}_e^m$, $\tilde{\mathbf{B}}_e^{b_1}$, $\tilde{\mathbf{B}}_e^{b_2}$, $\tilde{\mathbf{B}}_e^{s_0}$ and $\tilde{\mathbf{B}}_e^{s_1}$ are the smoothed bending and shear strain gradient matrices given by

$$\tilde{\mathbf{B}}^m = \frac{1}{A_e}\sum_{j=1}^{3} A_{\Delta_j}\mathbf{B}^{m\Delta_j} \quad ; \quad \tilde{\mathbf{B}}_e^{b_1} = \frac{1}{A_e}\sum_{j=1}^{3} A_{\Delta_j}\mathbf{B}^{b_1\Delta_j} \quad ; \quad \tilde{\mathbf{B}}_e^{b_2} = \frac{1}{A_e}\sum_{j=1}^{3} A_{\Delta_j}\mathbf{B}^{b_2\Delta_j}$$
$$\tilde{\mathbf{B}}_e^{s_0} = \frac{1}{A_e}\sum_{j=1}^{3} A_{\Delta_j}\mathbf{B}^{s_0\Delta_j} \quad ; \quad \tilde{\mathbf{B}}_e^{s_1} = \frac{1}{A_e}\sum_{j=1}^{3} A_{\Delta_j}\mathbf{B}^{s_1\Delta_j} \tag{26}$$

Therefore the global stiffness matrix of the CS-MIN3 are assembled by

$$\tilde{\mathbf{K}} = \sum_{e=1}^{N_e} \tilde{\mathbf{K}}_e \tag{27}$$

where $\tilde{\mathbf{K}}_e$ is the smoothed element stiffness for plate given by

$$\begin{aligned}\tilde{\mathbf{K}}_e &= \int_{\Omega_e} \tilde{\mathbf{B}}^T\mathbf{D}^*\tilde{\mathbf{B}}\,\mathrm{d}\Omega + \int_{\Omega_e} \tilde{\mathbf{S}}^T\mathbf{D}_s^*\tilde{\mathbf{S}}\,\mathrm{d}\Omega + \int_{\Omega_e} \mathbf{N}_w^T k_f \mathbf{N}_w\,\mathrm{d}\Omega \\ &= \tilde{\mathbf{B}}^T\mathbf{D}^*\tilde{\mathbf{B}}\,A_e + \tilde{\mathbf{S}}^T\mathbf{D}_s^*\tilde{\mathbf{S}}A_e + \int_{\Omega_e} \mathbf{N}_w^T k_f \mathbf{N}_w\,\mathrm{d}\Omega\end{aligned} \tag{28}$$

in which

$$\tilde{\mathbf{B}} = \left[\left(\tilde{\mathbf{B}}_e^m\right)^T \quad \left(\tilde{\mathbf{B}}_e^{b_1}\right)^T \quad \left(\tilde{\mathbf{B}}_e^{b_2}\right)^T\right] \quad ; \quad \tilde{\mathbf{S}} = \left[\left(\tilde{\mathbf{B}}_e^{s_0}\right)^T \quad \left(\tilde{\mathbf{B}}_e^{s1}\right)^T\right] \tag{29}$$

Note that for convenience in numerical computation, the foundation stiffness coefficient k_f in Eq. (28) can be derived from the following equation ref in [23]

$$k_f = KD/B^4 \tag{30}$$

where K is the non-dimensional elastic foundation coefficient; B is the shorter dimension of the plate; and $D = Et^3/\left(12(1-\nu)\right)$ is the bending stiffness of the plate.

4. TRANSFORMATION OF THE MOVING VEHICLE INTO THE LOAD AT NODES

In this section, a transformation of moving vehicle into the load at nodes is presented. First, some hypothesis of the model of loads and moving rule of vehicles are assumed as follows:

+ Model of loads: moving concentrated loads
+ Moving rule of vehicles on the plate: along the straight line with regular velocity

4.1. Transformation of the weight of a four-wheel vehicle into concentrated loads

In the literature, the forces of a vehicle on the plate are considered as concentrated loads. Here, we assume that the concentrated loads are located at the wheels of a four-wheel vehicle.

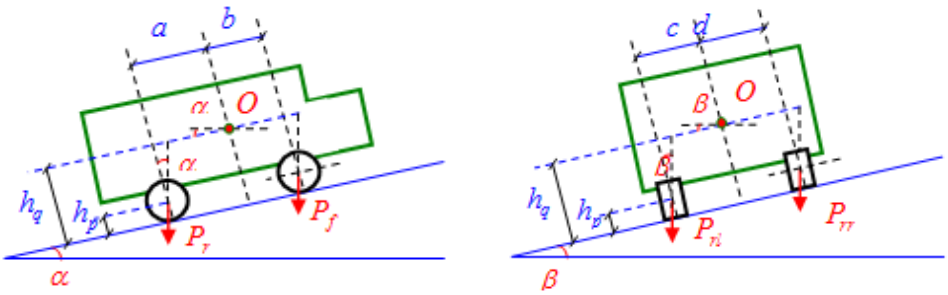

(a) (b)

Fig. 2. Distribution weight of vehicle to four wheels; (a) the longitudinal axis of the vehicle inclines an angles α compared with the surface of the plate; (b) the lateral axis of the vehicle inclines an angle β compared with the surface of the plate

Fig. 2 illustrates a simple model of a four-wheel vehicle moving on the plate, in which the longitudinal axis of the vehicle inclines an angles α compared with the surface of the plate, and the lateral axis of the vehicle inclines an angle β compared with the surface of the plate. Using the geometrical analysis, the concentrated loads at four wheels are now defined by

$$\begin{cases} P_{rl} = Q\left(1 - \dfrac{a - h_q\mathrm{tg}\alpha + h_p\mathrm{tg}\alpha}{a+b}\right)\left(1 - \dfrac{c - h_q\mathrm{tg}\beta + h_p\mathrm{tg}\beta}{c+d}\right) \\ P_{rr} = \dfrac{Q}{c+d}\left(1 - \dfrac{a - h_q\mathrm{tg}\alpha + h_p\mathrm{tg}\alpha}{a+b}\right)(c - h_q\mathrm{tg}\beta + h_p\mathrm{tg}\beta) \\ P_{fl} = \dfrac{Q}{a+b}(a - h_q\mathrm{tg}\alpha + h_p\mathrm{tg}\alpha)\left(1 - \dfrac{c - h_q\mathrm{tg}\beta + h_p\mathrm{tg}\beta}{c+d}\right) \\ P_{fr} = \dfrac{Q}{(a+b)(c+d)}(a - h_q\mathrm{tg}\alpha + h_p\mathrm{tg}\alpha)(c - h_q\mathrm{tg}\beta + h_p\mathrm{tg}\beta) \end{cases} \tag{31}$$

where Q is the weight of the vehicle; P_{rl}, P_{rr}, P_{fl} and P_{fr}, respectively, are the concentrated loads located at the rear-left wheel, the rear-right wheel, the front-left wheel and the front-right wheel; a and b, respectively, are the distances from the centre of the vehicle to the axis connecting two rear wheels and the axis connecting two front wheels; c and d, respectively, are the distances from the centre of the vehicle to the axis connecting two left wheels and the axis connecting two right wheels; h_q and h_p, respectively, are the distances from the plate surface to the centre of the vehicle and the centre of the wheels.

4.2. Transformation of the concentrated loads at the wheels into the load at nodes of elements

Using the CS-MIN3 for the analysis of Mindlin plates on viscoelastic foundation, the plate will be discretized into three-node triangular elements, and hence the concentrated loads at four wheels of the moving vehicle will be located on these triangular elements.

We hence need to transform the concentrated loads into the load at nodes of the elements at any time t.

Fig. 1c shows a model of a moving concentrated load P crossing triangular elements. In this model, the concentrated load P moves along the line inclined an angle θ compared with x axis. Suppose that at the time point t, the position of the moving concentrated load P is (a, b) in the Cartesian coordinate system Oxy. Then, the new position $(\bar{x}, \bar{y})$ of the moving concentrated load at the time $\bar{t} = t + \Delta t$ are defined as

$$\bar{x} = v\Delta t \cos\theta + a \; ; \quad \bar{y} = v\Delta t \sin\theta + b \tag{32}$$

where v is velocity of the moving vehicle and Δt is step time. The moving concentrated load P at the position $(\bar{x}, \bar{y})$ is then transformed into the force vector $\bar{\mathbf{F}}$ at nodes of elements by

$$\bar{\mathbf{F}} = P\mathbf{N}_w \tag{33}$$

in which $\mathbf{N}_w = [0\ 0\ N_1\ 0\ 0\ 0\ 0\ 0\ 0\ N_2\ 0\ 0\ 0\ 0\ 0\ 0\ N_3\ 0\ 0\ 0\ 0]$ is the vector of values of shape functions at the position $(\bar{x}, \bar{y})$ on the element containing the moving concentrated load; and P is one of four concentrated loads P_{fr}, P_{fl}, P_{rr}, P_{rl} introduced in the previous section.

An algorithm for determining the position of moving concentrated load P at the time $\bar{t} = t + \Delta t$ is briefly presented as follows:

Step 1: calculate coordinates of the vehicle according to Eq. (32).

Step 2: determine the elements which are containing the moving concentrated loads

Step 3: calculate the concentrated forces caused by the mass of vehicle

Step 4: transform these forces into the loads at nodes of elements according to Eq. (33).

5. NUMERICAL RESULTS

5.1. Static and free vibration analyses of Mindlin plate on the elastic foundation

Consider the static analysis of a rectangular plate rested on the elastic foundation with the non-dimensional elastic foundation coefficient given by $K = 1000$. This example was studied by Ref [23]. The plate is subjected to a concentrated load $P = 1000$ N at the center and the size of plate is given by length $L = 50$ m, width $B = 10$ m and thickness $t = 0.02$ m as shown in Fig. 3a. The plate is is free along two longer edges and is simply supported along the two remaining edges. The material parameters of plate are given by Young's modulus $E = 31 \times 10^9$ N/m^2 and Poisson's ratio $\nu = 0.2$. Four uniform discretizations of plate corresponding to 72, 200, 252 and 800 elements are used. The convergence of deflection is first studied. Fig. 3b compares the convergence of central deflection $\bar{w} = wD/(PB^2)$ of plate using the CS-MIN3 and others numerical methods such as MIN3, discrete shear gap method (DSG3) [24], mixed interpolated tensorial components (MITC4) [25]. The reference solution by Huang [23] is used. It is seen that the solution of the CS-MIN3 is the closest to the reference solution, even with coarse meshes.

Now, the free vibration analysis of the plate on the elastic foundation is considered. The plate model in Fig. 3a is still chosen to analysis, however in order to compare the

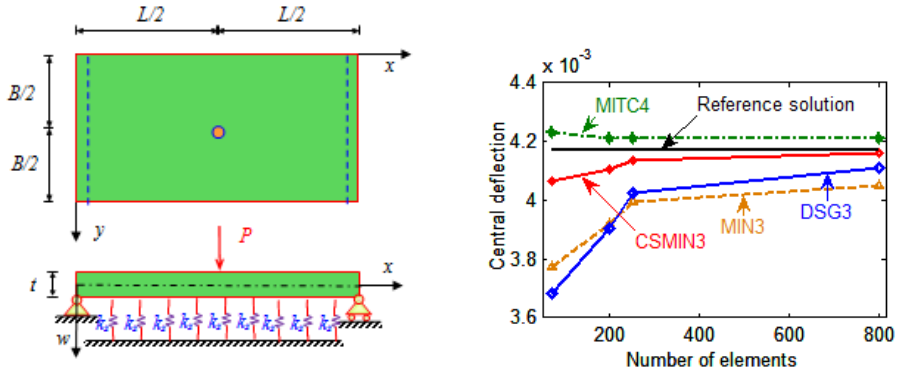

(a) (b)

Fig. 3. (a) Model of the plate resting on elastic foundation under a concentrated load at the center; (b) Convergence of central deflection $\bar{w} = wD/(PB^2)$ of plate

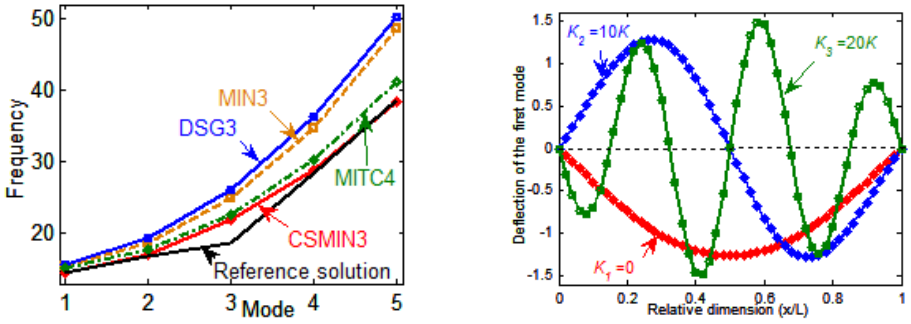

(a) (b)

Fig. 4. (a) Five lowest frequencies of the plate on elastic foundation; (b) Deflection of the first mode of the plate on the elastic foundation at middle line along the longitudinal direction x

results with those from Huang (2001), the dimensions of the plate are reset into the length $L = 30$ m, the width $B = 10$ m, the thickness $t = 0.5$ m and the boundary conditions of plate are changed into being simply supported along four edges of plate. The density of plate is given by $\rho = 2500$ kg/m^3 and the foundation coefficient is reset into $K = 100$. Fig. 4a plots five lowest frequencies of plate by different numerical methods for the meshes 15×5. It is observed that the results of CS-MIN3 agree well with the reference solution of Huang [23] and are much more accurate than those of the others elements. In particular, the CS-MIN3 can provide accurately the values of high frequencies of plates by using only coarse meshes. We next study the deflection of free vibration modes of the plate on the elastic foundation corresponding to three sets of various foundation coefficients: $K_1 = 0$ (without foundation), $K_2 = 10K$ and $K_3 = 20K$. Fig. 4b plots the deflection of the first

free vibration modes of the plate on the elastic foundation at the middle line ($y = 5$ m) along the longitudinal direction x. It can be seen that when the stiffness of foundation becomes stiffer, the deflections of modeshape of the plate on the elastic foundation change significantly comparing with those of the plate without foundation.

5.2. Dynamic analysis of Mindlin plate on viscoelastic foundations under to a moving vehicle

We now consider a four-wheel vehicle moving with velocity $v = 50$ m/s on the middle line along the longitudinal direction x of a rectangular plate as shown in Fig. 5a. The rectangular plate is simply supported along two shorter sides, and free along two longer sides. The mass of the vehicle is $M = 1000$ kg. The material parameters of the plate are given by Young's modulus $E = 3.1 \times 10^{10}$ N/m^2, Poisson's ratio $\nu = 0.2$, the length $L = 20$ m, the width $B = 10$ m, the thickness $t = 0.3$ m and the density mass $\rho = 1000$. The parameters of the foundation are given by the foundation coefficient $K = 1000$ and the damping coefficient $c_f = 5 \times 10^5$ Ns/m^2.

We first study the difference of the deflection of the plate for two cases: a) the vehicle weight is transformed into four concentrated loads at four wheels (L4); and b) the vehicle weight is transformed into only one concentrated load located at the central point of four wheels (L1).

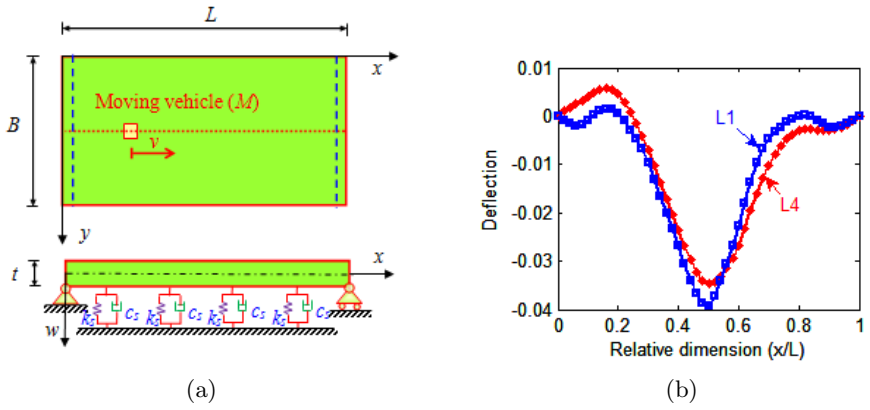

Fig. 5. (a) Models of rectangular plate resting on viscoelastic foundation under a moving vehicle; (b) Deflection of middle line by CS-MIN3 (car at the middle of plate)

Fig. 5b shows the variation of the deflection of the plate along the middle line by CS-MIN3 when the vehicle moves to the middle of the plate. The results show that the deflections of the plate by L4 are considerably smaller than those of by L1. This hence implies that it is necessary to transform the vehicle weight into the concentrated loads at the wheels to ensure the accuracy the analyzed results.

Next, we conduct the parametric study to determine the effects of various parameters on the dynamic response of the plates on the viscoelastic foundation subjected to

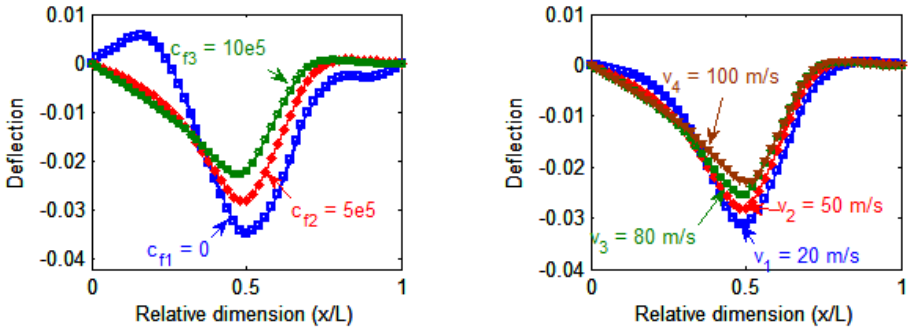

(a) (b)

Fig. 6. (a) Deflection of middle line with various damping coefficients; (b) Deflection of middle line of the plate with various velocity of moving vehicle

the moving vehicle. The variation of the deflection of the plate along the middle line by CS-MIN3, together the scheme of load transformation L4, is examined. First, three various damping coefficients are considered, $c_{f1} = 0$, $c_{f2} = 5 \times 10^5$ Ns/m^2 and $c_{f3} = 10 \times 10^5$ Ns/m^2, and the results are shown in Fig. 6a. It is observed that when the damping coefficient increases, the deflection becomes smaller, as expected, and the shape of deflection also changes significantly. Finally, four various velocities of the moving vehicle are considered, $v_1 = 20$ m/s, $v_2 = 50$ m/s, $v_3 = 80$ m/s and $v_3 = 100$ m/s, and the results are shown in Fig. 6b. It is shown that when the velocity of moving vehicle becomes faster, the deflection of the plate becomes smaller, as expected, and the shape of deflection also changes significantly.

6. CONCLUSIONS

The paper presents an incorporation of the CS-MIN3 based on C0-type higher-order shear deformation theory (HSDT) with damping-spring systems for dynamic analyses of Mindlin plates on the visco-elastic foundation subjected to a moving vehicle. The Mindlin plate-foundation system is modeled as a discretization of triangular plate elements supported by discrete springs and dashpots at the nodal points representing the viscoelastic foundation. A two-step process for transforming the weight of a four-wheel vehicle into loads at nodes of elements is presented. Through the present formulation and numerical results, we can withdraw some advantages of CS-MIN3 as follows:

i) The proposed CS-MIN3 only uses three-node triangular elements that are much easily generated automatically for complicated geometry domains.

ii) By using seven degrees of freedom at each vertex node, the CS-MIN3 using C^0-HSDT can be considered as an C^1-HSDT continuity element.

iii) Due to using the gradient smoothing technique which can help soften the over-stiff behavior in the MIN3, the proposed CS-MIN3 improves significantly the accuracy of the numerical results.

iv) The high accuracy and fast convergence of the proposed CS-MIN3 are verified by comparing its numerical solutions with those of others available numerical results (such as MIN3, DSG3, MITC4).

v) Analyses of the effects of various parameters on the dynamic response of the plates on the viscoelastic foundation subjected to the moving vehicle by the CS-MIN3 give the expected results.

ACKNOWLEDGEMENTS

This work was supported by Vietnam National Foundation for Science & Technology Development (NAFOSTED), Ministry of Science & Technology, under the basic research program (Project No.:107.02-2012.05).

REFERENCES

[1] R. S. Ayre, L. S. Jacobson, and C. S. Hsu. Transverse vibration of one and two-span beam under the action of a moving mass load. In *Proceedings of the First U.S. National Congress of Applied Mechanics*, (1951), pp. 81–90.

[2] D. Yoshida and W. Weaver. Finite element analysis of beams and plates with moving loads. *Publication of International Association for Bridge and Structural Engineering*, **31**(1), (1971), pp. 179–195.

[3] J. Kenney. Steady-state vibrations of beam on elastic foundation for moving load. *Journal of Applied Mechanics-Transactions of the ASME*, **21**(4), (1954), pp. 359–364.

[4] W. E. Thompson. Analysis of dynamic behavior of roads subject to longitudinally moving loads. *HRB*, **39**, (1963), pp. 1–24.

[5] M. Zaman, M. R. Taheri, and A. Alvappillai. Dynamic response of a thick plate on viscoelastic foundation to moving loads. *International journal for numerical and analytical methods in geomechanics*, **15**(9), (1991), pp. 627–647.

[6] L. Sun. Dynamic response of Kirchhoff plate on a viscoelastic foundation to harmonic circular loads. *Journal of applied mechanics*, **70**(4), (2003), pp. 595–600.

[7] G.-R. Liu and N. T. Trung. *Smoothed finite element methods*. CRC Press, (2010).

[8] J.-S. Chen, C.-T. Wu, S. Yoon, and Y. You. A stabilized conforming nodal integration for Galerkin mesh-free methods. *International Journal for Numerical Methods in Engineering*, **50**(2), (2001), pp. 435–466.

[9] G. R. Liu, K. Y. Dai, and T. T. Nguyen. A smoothed finite element method for mechanics problems. *Computational Mechanics*, **39**(6), (2007), pp. 859–877.

[10] H. Nguyen-Xuan and T. Nguyen-Thoi. A stabilized smoothed finite element method for free vibration analysis of Mindlin–Reissner plates. *Communications in Numerical Methods in Engineering*, **25**(8), (2009), pp. 882–906.

[11] T. Nguyen-Thoi, T. Bui-Xuan, P. Phung-Van, S. Nguyen-Hoang, and H. Nguyen-Xuan. An edge-based smoothed three-node Mindlin plate element (ES-MIN3) for static and free vibration analyses of plates. *Civ. Eng*, (2013).

[12] T. Nguyen-Thoi, P. Phung-Van, H. Nguyen-Xuan, and C. Thai-Hoang. A cell-based smoothed discrete shear gap method using triangular elements for static and free

vibration analyses of Reissner–Mindlin plates. *International journal for numerical methods in Engineering*, **91**(7), (2012), pp. 705–741.

[13] T. Nguyen-Thoi, P. Phung-Van, C. Thai-Hoang, and H. Nguyen-Xuan. A cell-based smoothed discrete shear gap method (CS-DSG3) using triangular elements for static and free vibration analyses of shell structures. *International Journal of Mechanical Sciences*, **74**, (2013), pp. 32–45.

[14] T. Nguyen-Thoi, T. Bui-Xuan, P. Phung-Van, H. Nguyen-Xuan, and P. Ngo-Thanh. Static, free vibration and buckling analyses of stiffened plates by CS-FEM-DSG3 using triangular elements. *Computers & Structures*, **125**, (2013), pp. 100–113.

[15] P. Phung-Van, T. Nguyen-Thoi, L. Tran-Vinh, and H. Nguyen-Xuan. A cell-based smoothed discrete shear gap method (CS-DSG3) based on the C0-type higher-order shear deformation theory for static and free vibration analyses of functionally graded plates. *Computational Materials Science*, **79**, (2013), pp. 857–872.

[16] P. Phung-Van, T. Nguyen-Thoi, T. Le-Dinh, and H. Nguyen-Xuan. Static and free vibration analyses and dynamic control of composite plates integrated with piezoelectric sensors and actuators by the cell-based smoothed discrete shear gap method (CS-FEM-DSG3). *Smart Materials and Structures*, **22**(9), (2013), p. 095026.

[17] T. Nguyen-Thoi, P. Phung-Van, T. Rabczuk, H. Nguyen-Xuan, and C. Le-Van. An application of the ES-FEM in solid domain for dynamic analysis of 2D fluid–solid interaction problems. *International Journal of Computational Methods*, **10**, (01), (2013).

[18] T. Nguyen-Thoi, P. Phung-Van, T. Rabczuk, H. Nguyen-Xuan, and C. Le-Van. Free and forced vibration analysis using the n-sided polygonal cell-based smoothed finite element method (nCS-FEM). *International Journal of Computational Methods*, **10**, (01), (2013).

[19] T. Nguyen-Thoi, P. Phung-Van, H. Luong-Van, H. Nguyen-Van, and H. Nguyen-Xuan. A cell-based smoothed three-node Mindlin plate element (CS-MIN3) for static and free vibration analyses of plates. *Computational Mechanics*, **51**(1), (2013), pp. 65–81.

[20] A. Tessler and T. J. Hughes. A three-node Mindlin plate element with improved transverse shear. *Computer Methods in Applied Mechanics and Engineering*, **50**(1), (1985), pp. 71–101.

[21] C. Shankara and N. Iyengar. A C^0 element for the free vibration analysis of laminated composite plates. *Journal of Sound and Vibration*, **191**(5), (1996), pp. 721–738.

[22] J. N. Reddy. A simple higher-order theory for laminated composite plates. *Journal of applied mechanics*, **51**(4), (1984), pp. 745–752.

[23] M.-H. Huang and D. Thambiratnam. Analysis of plate resting on elastic supports and elastic foundation by finite strip method. *Computers & Structures*, **79**(29), (2001), pp. 2547–2557.

[24] K.-U. Bletzinger, M. Bischoff, and E. Ramm. A unified approach for shear-locking-free triangular and rectangular shell finite elements. *Computers & Structures*, **75**(3), (2000), pp. 321–334.

[25] K.-J. Bathe and E. N. Dvorkin. A four-node plate bending element based on Mindlin/Reissner plate theory and a mixed interpolation. *International Journal for Numerical Methods in Engineering*, **21**(2), (1985), pp. 367–383.

VIETNAM ACADEMY OF SCIENCE AND TECHNOLOGY
VIETNAM JOURNAL OF MECHANICS VOLUME 36, N. 1, 2014

CONTENTS